Journal of Diabetes and Its Complications 33 (2019) 148–159

Contents lists available at ScienceDirect

Journal of Diabetes and Its Complications

journal homepage: WWW.JDCJOURNAL.COM

Low proliferative potential of adipose-derived stromal cells associates with hypertrophy and inflammation in subcutaneous and omental adipose tissue of patients with type 2 diabetes mellitus

I. Stafeev [a,b,c,*], N. Podkuychenko [a,b,c], S. Michurina [a,b], I. Sklyanik [c], A. Panevina [c], E. Shestakova [c], K. Yah'yaev [d], V. Fedenko [e], E. Ratner [a,c], A. Vorotnikov [a], M. Menshikov [a], Y. Yashkov [e], Ye. Parfyonova [a,b,1], M. Shestakova [c,1]

[a] National Medical Research Centre for Cardiology, Moscow, Russia
[b] M.V. Lomonosov Moscow State University, Moscow, Russia
[c] Endocrinology Research Centre, Moscow, Russia
[d] Central Clinical Hospital #1 of LLC Russian Railways, Moscow, Russia
[e] V.I. Kulakov National Medical Research Centre for Obstetrics, Gynecology and Perinatology, Moscow, Russia

ARTICLE INFO

Article history:
Received 6 August 2018
Received in revised form 25 September 2018
Accepted 16 October 2018
Available online 4 November 2018

Keywords:
ADSC
Type 2 diabetes mellitus
Insulin resistance
Inflammation

ABSTRACT

Background: Obesity and type 2 diabetes mellitus (T2DM) are among the most important morbidity factors. In this study we tested the hypothesis that low proliferative potential of adipose derived stromal cells (ADSC) associates with reduced formation of new fat depots, excess accumulation of fat in the functional adipocytes and their hypertrophy, resulting in fat inflammation and insulin resistance.
Methods: We screened two groups of obese patients with or without T2DM, matched for BMI, age, and duration of obesity to test the hypothesis that hypertrophy and decreased renewal of adipocytes may underlie transition from obesity to T2DM. All patients were matched for carbohydrate metabolism (fasting blood glucose level, glycated hemoglobin, HOMA-IR index and M-index). The subcutaneous and omental fat tissue biopsies were obtained during bariatric surgery from obese individuals with or without T2DM. The morphology and immunophenotype of subcutaneous and omental fat was assessed in frozen tissue sections. ADSC were isolated from both types of fat tissue biopsies and screened for morphology, proliferative potential and inflammatory status.
Results: The non-diabetic patients had normal carbohydrate metabolism and moderate insulin resistance measured by HOMA-IR and hyperinsulinemic clamp (M-index), while T2DM patients were extremely insulin resistant by both indexes. The average size of diabetic adipocytes was higher than that of non-diabetic in both subcutaneous and omental fat tissues, indicating adipocyte hypertrophy in T2DM. Both these tissues contained higher level of macrophage infiltration and increased M1-like to M2-like ratio of macrophage subpopulations, suggesting increased fat inflammation in T2DM. This was confirmed by increased activatory phosphorylation of stress-induced JNK1/2 in diabetic ADSC.
Conclusion: These results suggest that blunted proliferation and increased hypertrophy of diabetic ADSC may lead to reduced insulin sensitivity via increased inflammation mediated by M1 macrophages and JNK1/2 pathway.

1. Introduction

Obesity and metabolic disorders contribute to the health risk and morbidity in the contemporary society. Obesity closely associates with, and increases the risk of type 2 diabetes mellitus (T2DM), however not all of the obese individuals develop T2DM.[1] The mechanisms linking obesity to T2DM have been extensively studied including distorted lipid metabolism, oxidative stress, unfolded protein response, and inflammation, which appear to be a hallmark of all these events.[2–7]

Latent inflammation is critical to the onset of insulin resistance, particularly in adipose tissue. Cells exposed to nutrient excess such as high-fat diet become overfed and hypoxic, increase adipocyte size, exhibit

Abbreviations: T2DM, type 2 diabetes mellitus,; ADSC, adipose derived stromal cells; HOMA-IR index, homeostatic model assessment for insulin resistance; JNK, c-Jun NH_2-terminal kinase; NF-kB, nuclear factor kB; TNFα, tumor necrosis factor α; IL, interleukin; NGT, normal glucose tolerance; BMI, body mass index; sWAT, subcutaneous white adipose tissue; oWAT, omental white adipose tissue; DMEM, Dulbecco modified Eagle medium; FBS, fetal bovine serum; BSA, bovine serum albumin; FACS, fluorescence-activated cell sorting; HbA1c, glycated hemoglobin; CD, cluster of differentiation; CCR7, C-C chemokine receptor type 7; IR, insulin resistance.

* Corresponding author at: National Medical Research Centre for Cardiology, Moscow, Russia.
E-mail address: yuristafeev@gmail.com (I. Stafeev).

[1] These authors have equal contributions.

https://doi.org/10.1016/j.jdiacomp.2018.10.011
1056-8727/

oxidative stress and unfolded protein response, leading to activation of inflammatory NF-kB pathway.[8–10] These experimental results are in agreement with clinical studies that demonstrated high levels of different blood inflammatory cytokines such as TNFα, IL-1β, IL-6, IL-8,[11–13] and high infiltration of adipose tissue by immune cells.[14–16] However, as in the case of T2DM, obesity does not always precede inflammation in clinical observations.[14,17]

We hypothesized that inflammation and insulin resistance may occur independently of morbid obesity due to dysfunction of adipose-derived stromal cells (ADSC) in both subcutaneous and visceral fat. These cells have immune-privileged status and immunomodulatory capacity.[18–20] Systemic injection of ADSC from healthy animals to animals with diet-induced insulin resistance improved insulin sensitivity predominantly via phenotype modulation of adipose resident immune cells.[21–24] On the contrary, insulin resistance alters properties of ADSC to promote development of T2DM.[25,26] Thus, we expect that insulin resistance can be associated with disturbed function of ADSC. It has been shown that insulin resistance in obese subjects indeed associates with increased ADSC inflammation,[27] but other mechanisms linking ADSC to insulin resistance remain unclear.

In this study we tested the hypothesis that low proliferative potential of ADSC from obese patients associates with disturbed formation of new fat depots, resulting in excess accumulation of fat in functional fat depots, subsequent hypertrophy of adipocytes and inflammation of adipose tissue, leading to insulin resistance.

2. Materials and methods

The study was approved by Endocrinology Research Centre ethics committee (protocol #9 from 10 May 2017). Written informed consent was obtained from each of the volunteers.

2.1. Subjects

Five obese but otherwise healthy patients (normal glucose tolerance, NGT) and five obese T2DM patients were included in the study. All patients had long (>15 years) and morbid (BMI > 35 kg/m^2) obesity. Subjects <18 years old, with any other type of diabetes, pregnancy, cancer or inflammation were excluded from the study. The NGT patients were not taking any antidiabetic medicine. The T2DM patients were taking metformin ($n = 4$); dipeptidyl peptidase type 4 inhibitors ($n = 4$); sulfonylurea ($n = 2$); and sodium-glucose cotransporter type 2 inhibitors ($n = 1$). Subcutaneous (sWAT) and omental (oWAT) white adipose tissue biopsies, and the venous blood samples for standard clinical tests were obtained from patients during bariatric surgery after overnight fast.

2.2. Clinical characterization

Fasting glucose was measured with Architect c4000 clinical chemistry analyzer (Abbott Diagnostics, Abbott Park, IL, USA) using standard kits offered by the manufacturer. Glycated hemoglobin (HbA1c) was assessed with high-performance liquid chromatography (D-10 Hemoglobin Testing System, BioRad, France). All the patients also had body composition measurements taken (Tanita MC-780MA Body Composition Analyzer, TANITA Corporation, Japan). Adiponectin and leptin serum levels were measured by ELISA kits (Mercodia, Sweden) and optical density was revealed by microplate reader 1420 Multilabel Counter Victor2 (PerkinElmer, USA).

2.3. Insulin resistance

Insulin resistance was measured by two methods: HOMA-IR calculator and hyperinsulinemic-euglycemic clamp test. The HOMA-IR was calculated by the formulae:

$$\text{Insulin resistance} = \text{FI} \times \text{G}/22,5$$
$$\text{FI} = \text{fasting insulin level } (\mu\text{IU/ml})$$
$$\text{G} = \text{fasting glucose level } (\text{mmol/l})$$

The classic DeFronzo hyperinsulinemic-euglycemic clamp test was used to assess insulin resistance (IR).[30] Briefly, insulin was continuously infused at 100 μU/ml to inhibit systemic insulin secretion by the pancreas and liver. Simultaneously, 20% glucose was intravenously infused to reach normal blood level that was subsequently maintained by controlled infusion rate using Infusomat FMS volumetric infusion pump (B. Braun, Germany). The insulin infusion rate was set to 1 mU/kg/min using Perfusor compact syringe pump (B. Brown, Germany). Blood glucose was measured each 5–10 min with One Touch Verio Pro+ glucometer (Life Scan, Switzerland). The euglycemic option was chosen in order to mitigate the effects of hyperglycemia on glucose uptake. The target blood glucose levels were 5.1–5.6 mmol/l. If blood glucose decreased, glucose infusion was accelerated, and vice versa. In about 120–180 min, a dynamic equilibrium was achieved meaning that glucose infusion rate was equal to glucose uptake by the tissues. The glucose infusion rate at a dynamic equilibrium over 30–40 min was considered to be the glucose uptake by tissues and used to calculate glucose consumption (M value) as a mean of 6–8 glucose infusion rate readings per kg of body mass per minute. The results were expressed as M values (mg/kg/min) and classified as follows: M = 0–2, severe IR, M = 2–4, moderate IR, M = 4–6, mild IR, M > 6, no IR.

2.4. ADSC isolation and cell culture

ADSC were isolated from subcutaneous and omental white adipose tissue biopsies as previously described.[21] Briefly, the stromal vascular cell fraction was isolated by collagenase I (200 U/ml, Sigma-Aldrich, USA) and dispase (30 U/ml, Gibco, USA) digestion for 1 h at 37 °C. The cells were seeded and cultured overnight in complete DMEM supplemented by 10% FBS (HyClone, USA), PenStrep and 2 mM glutamine (Gibco, USA) followed by exchange of the medium to remove non-adherent cells. Experiments for cell proliferation assay were performed at 3rd passage. All experiments were performed using independent ADSC cultures from five obese non-diabetic patients and five obese patients with T2DM.

2.5. MTT assay

MTT was used in ADSC proliferation assay. The assay is based on conversion of water soluble MTT (3-(4,5-dimethylthiazol-2-yl)-2,5-diphenyltetrazolium bromide) compound to an insoluble formazan product by viable cells. Optical absorbance by formazan at 590 nm is proportional to the number of cells. Proliferative index was determined as (number of cells (+FBS sample)/number of cells (−FBS sample)). ADSC were plated in 96-well culture plates ($5 * 10^3$ cells per well) in complete DMEM supplemented with 10% FBS in a final volume of 0.1 ml. The cells were serum-deprived in complete DMEM and 0.1% BSA overnight prior to experiments and cultured for 24, 48, 72 and 96 h in complete DMEM with or without 10% FBS. Then MTT was added at 0.5 mg/ml for 4 h. Formazan crystals were solubilized by 0.1 N HCl in isopropanol. Absorbance was measured at 595 nm using Multiscan Microplate Reader (Labsystems, USA) and number of cells per well was calculated using standard curves. The standard calibration curves (absorbance against the number of cells) were generated using 6 serial dilutions from 620 to 20,000 cells/well.

2.6. Cell cycle assay

A flow cytometry based cell cycle assay was performed using Propidium Iodide Flow Cytometry Kit (ab139418, Abcam, UK) to

evaluate distribution of ADSC over cell cycle. Cells were cultured for 24 h in complete DMEM with or without 10% FBS, detached and fixed in an ice-cold 70% ethanol for 4 h. DNA was denaturated by 2 N HCl with 0.5% Triton-X100, and solution was neutralized to pH 8.5 with 0.1 M borate buffer. The cells were washed and resuspended in 50 mg/ml propidium iodide (Abcam, UK) supplemented with 550 U/ml RNase A (Abcam, UK). FACS Canto II (BD Pharmingen, USA) was used for flow cytometry. FCS Express 9 software (De Novo Software, Canada) was used to analyze cell distribution over the phases of the cell cycle based on intensity of propidium iodide fluorescence.

2.7. Adipocyte area measurements

The average area covered by adipocytes was determined by the bright field microscopy of frozen sections of sWAT and oWAT biopsies. The biopsies were immersed in freezing medium (O.C.T. Tissue Tek, Sakura, Japan) and frozen in vapor of liquid N_2. They were cut into series of 30 μm thick sections that were transferred onto glass slides and fixed in ice-cold acetone. The sections were dehydrated in 96% ethanol and xylene and visualized on a microscope Zeiss Axio Observer A1 (Zeiss, Germany). The images were analyzed using ImageJ software (SetScale plugin). The average adipocyte area were determined from 4 randomized microscopic fields and counted as total area covered by adipocytes divided by the number of cells examined.

2.8. Immunohistochemistry

Frozen Tissue Tek blocks of sWAT and oWAT were cut into 12 μm thick sections and fixed in ice-cold acetone. All sections were blocked by 10% normal donkey serum and incubated overnight with primary antibodies (anti-CD68-antibody, #ab955, Abcam, USA; anti-CCR7-antibody, #ab32527, Abcam, USA; anti-CD206-antibody, #ab64693, Abcam, USA). The conjugated AlexaFluor488 (#A21206, Molecular Probes, USA) or AlexaFluor594 (#A21203, Molecular Probes, USA) were used as secondary antibody; all sections were counterstained with DAPI (Sigma-Aldrich, USA). The images were obtained on a fluorescent microscope Zeiss AXIO Observer A1 (Zeiss, Germany) and analyzed using ImageJ software. Percentage of macrophages was determined as number of $CD68^+$-cells among general number of cells. Percentage of M1-M2 macrophages was determined as number of $CD68^+$M1-M2 $marker^+$ cells among $CD68^+$-cells.

2.9. Adipogenic differentiation

Adipogenic differentiation was performed according to Zebisch et al.[28] Briefly, ADSC were cultured to 90% confluency in DMEM as above; the medium was then replaced with DMEM+10% newborn calf serum (NBCS) (days 0–2 of differentiation). On day 3, the medium was replaced with DMEM supplemented with 10% FBS, 0.5 mM dexamethasone, 0.25 μM isobutylmethylxanthine, 2uM rosiglitazone and 1 μg/ml insulin (days 3–5 of differentiation). The cells were cultured for another two days (days 5–7 of differentiation) in DMEM supplemented with 10% FBS and 1 μg/ml insulin. Then medium were replaced according to scheme: 2 days DMEM + full inductors, 2 days DMEM + insulin. On day 21, the cells were lysed and used in Western blotting. Control of adipogenic differentiation was performed by OilRedO staining, almost 80% of cells were OilRedO-positive.

2.10. Western blotting

Cell lysates were separated by Laemmli SDS-PAGE[29] and proteins were transferred on PVDF membranes at 1 A/h. The membranes were blocked for 5% fat-free milk in TBS containing 0.1% Tween 20 (TBST) and incubated with primary (anti-pJNK1/2 T183/Y185 antibody, cat. #AF1205, R&D, USA; anti-total JNK1/2 antibody, cat.#AF1387, R&D, USA; anti-vinculin antibody, cat.#ab129002, Abcam, USA) and secondary (horseradish peroxidase-conjugated secondary antibody against rabbit IgG, cat.#6721, Abcam, USA) antibodies according to manufacturer recommendations. The protein bands were visualized using Clarity ECL reagent kit (BioRad, USA) and Fusion FX gel-documenting system (Vilber Lourmat, France). Quantitation was performed in GelAnalyzer2010 software.

2.11. Gene expression studies

Expression of the key adipogenic markers *GLUT4*, *PPARgamma* and *FABP4* was measured by quantitative RT-PCR (PCR-system StepOnePlus, Applied Biosystems, USA) in the lysates of adipocytes derived from ADSC. Total RNA was purified from cell lysates using RNEasy Mini Kit (Qiagen, USA). The purified RNA was treated with DNase (Abcam, USA) and cDNA synthesis was performed using RevertAid H Minus First Strand cDNA Synthesis Kit (Thermo Scientific, USA). A SYBR-green based gene expression assay was performed by RT PCR Kit (Sintol, Russia). All samples were assayed in triplicates and values were compared against the housekeeping gene *GAPDH*. The mRNA level was quantified by 2^(−ΔΔCt) method (Table 1).

2.12. Statistical analysis

The data in Table 2 were expressed as median [max.; min.]. After that, all data were expressed as mean ± standard error of the mean (SEM) and analyzed using "Statistica 8.0" software. Statistically significant differences between two groups were evaluated by the Mann-Whitney rank sum *U* test. The *p*-values <0.05 were considered significant.

3. Results

3.1. Clinical characteristics of patients

General characteristics of the patients enrolled in the study are summarized in Table 2. The median fasting glucose was 8.56 [6.87; 11.57] mmol/l and median HbA1c was 7.40 [6.65; 8.10] % in T2DM patients; the median fasting glucose was 4.98 [4.77; 5.83] mmol/l and median HbA1c was 5.40 [5.20; 5.80] % in NGT patients, $p < 0.05$. The body mass index values did not differ between the two groups being 42.26 [34.83; 46.75] kg/m^2 in obese diabetic (T2DM) vs. 44.25 [36.27; 53.46] kg/m^2 in obese non-diabetic (NGT) patients. The groups differed in body composition as assessed by the adipose tissue vs. muscle tissue ratio. NGT patients had more adipose tissue (44%) than T2DM patients (41%). There was more visceral fat in T2DM patients (20.0 level [red area]) than in NGT patients (16.0 level [yellow area], $p = 0.032$). This suggests that fat was somewhat distributed towards the metabolically inactive form in T2DM patients.

The blood serum levels of adipokines have been also assessed. The T2DM patients had reduced adiponectin levels (NGT vs. T2DM: 6.67 [5.63; 9.00] vs. 4.36 [3.55; 5.24], $p = 0.016$) and a tendency to increased leptin level (NGT vs. T2DM: 26.53 [13.85; 40.00] vs. 41.25 [34.68; 53.50], $p = 0.151$) (Table 2).

3.2. Insulin resistance in patients

IR was measured by clamp test in all patients enrolled in the study. The M value was 1.23 [0.61; 1.57] mg/kg/min in T2DM patients vs. 4.14

Table 1
Sequences of primers for RT PCR.

Gene	Forward primer 5′-3′	Reverse primer 5′-3′
hGLUT4	CGTCTCCATTGTGGCCATCT	CCCATAGCCTCCGCAACATA
hPPARg	TCAAAGTGGAGCCTGCATCT	TGAGACATCCCCACTGCAAG
hFABP4	GCACCATAACCTTAGATGGGGG	GTGACGCCTTTCATGACGC
hGAPDH	CTCATTTCCTGGTATGACAACGA	CTTCCTCTTGTGCTCTTGCT

Table 2
Characteristics of carbohydrate metabolism in obese patients with and without T2DM (median [25,75 percentile]).

Characteristic	NGT patients	T2DM patients
Sex	4 females + 1 male	4 females + 1 male
Age, years	33 [29; 44]	42 [35; 59]
BMI, kg/m^2	44.25 [36.27; 53.46]	42.26 [34.83; 46.75]
Fasting blood glucose, mmol/l	4.98 [4.77; 5.83]	8.56 [6.87; 11.57]
HbA1c, %	5.40 [5.20; 5.80]	7.40 [6.65; 8.10]
HOMA-IR index	4.21 [1.64; 8.23]	13.23 [8.36; 20.33]
M-index, mg/kg/min	4.14 [3.44; 5.75]	1.23 [0.61; 1.57]
Serum adiponectin, μg/ml	6.67 [5.63; 9.00]	4.36 [3.55; 5.24]
Serum leptin, ng/ml	26.53 [13.85; 40.00]	41.25 [34.68; 53.50]

[3.44; 5.75] mg/kg/min in NGT patients, $p = 0.009$. This corresponds to severe IR in T2DM patients and mild to moderate IR in NGT patients.

3.3. Adipocytes are hypertrophied in obese diabetic vs. non-diabetic patients

Both subcutaneous and omental fat tissue biopsy were obtained from 5 each of NGT and T2DM patients. The average adipocyte area of subcutaneous WAT adipocytes in histological sections of T2DM biopsies was 1.5-fold larger than that of NGT biopsies (Fig. 1A–B) (2812 μm^2 ± 209 μm^2 for T2DM patients and 2003 μm^2 ± 128 μm^2 for NGT patients, $^*p < 0.01$, Mann-Whitney *U* test). Similarly, average adipocyte area of omental WAT adipocytes was 1.2-fold larger in diabetic biopsies than in the control group (Fig. 1C–D) (2224 um^2 ± 142 μm^2 for T2DM patients and 1897 um^2 ± 100 μm^2, ** $0.01 < p < 0.05$, Mann-Whitney U test). This indicates that both sWAT and oWAT diabetic adipocytes of are hypertrophied as compared to non-diabetic adipocytes.

3.4. Diabetic ADSC display lower proliferative activity than non-diabetic ADSC

Because adipocyte hypertrophy may results from a deficit of lipid stores due to compromised proliferation and renewal of adipocytes in disease, we used MTT to assess proliferation activity of ADSCs. Upon stimulation by FBS, diabetic ADSC displayed shallow growth dynamics in culture and the number of cells was always 2–5-fold less than in corresponding non-diabetic control cells (Fig. 2A,B). Consistent with this observation, FBS significantly increased the number of non-diabetic subcutaneous ADSC in G2/S phase of the cell cycle, whereas it had no such effect on diabetic cells 24 h after the stimulation (Fig. 2C). Although no significant difference was found for the omental ADSC in G2/S phase (Fig. 2D), this may reflect a considerable lag-phase in their growth curves that start to separate only at 45–72 h post-stimulation (Fig. 2B).

3.5. Diabetic ADSC display lower adipogenic activity than non-diabetic ADSC

The blunted proliferation of diabetic ADSC may be associated with their lower adipogenic activity. Therefore we compared the adipogenic capacity of ADSC from the NGT and T2DM patients. First, we analyzed the ADSC adipogenic activity by OilRedO staining of the resulting adipocytes. While the adipocytes derived from ADSC of the NGT patients demonstrated >80% of differentiated cells containing small lipid droplets, the adipocytes derived from ADSC of the T2DM patients demonstrated only 40–50% differentiated cells with hypertrophied morphology and

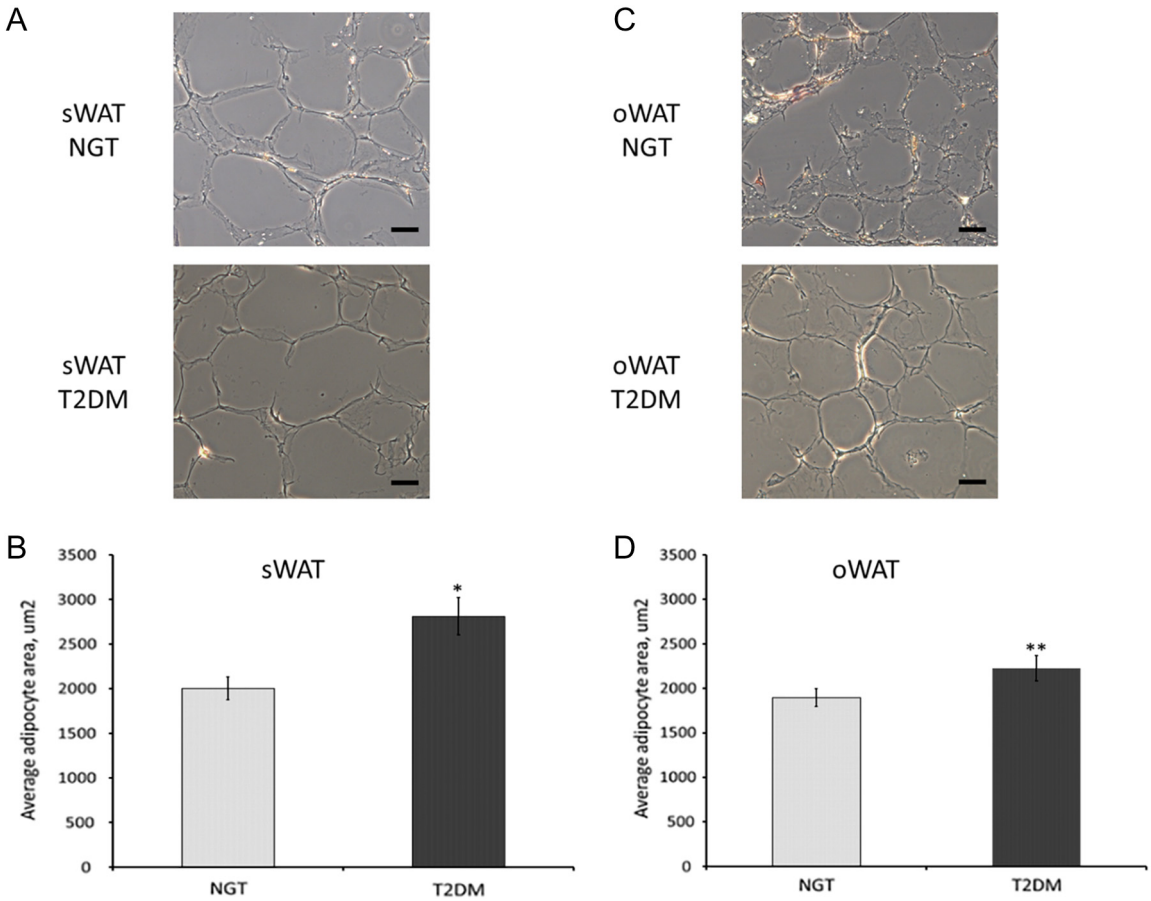

Fig. 1. Both subcutaneous (sWAT) and omental (oWAT) diabetic adipocytes (T2DM) are larger than non-diabetic adipocytes (NGT) in white adipose tissue biopsies. A, representative images of sWAT cryosections; B, average adipocyte areas for sWAT; C, representative images of oWAT cryosections, D, average adipocyte areas for oWAT. The data in histograms are Mean ± SEM, $n = 20$, Mann-Whitney *U* test. * - $p < 0.01$, ** - $0.01 < p < 0.05$. Scale bar = 20 μm.

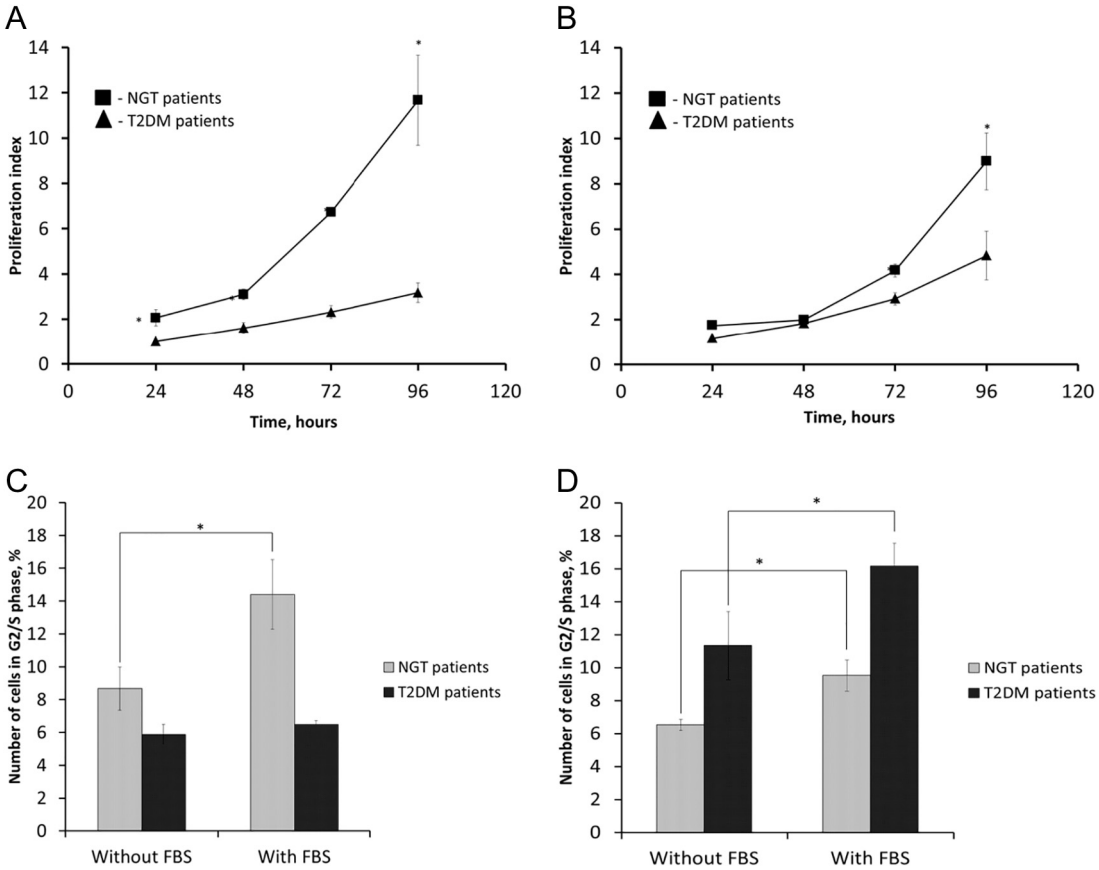

Fig. 2. Diabetic ADSC (T2DM) proliferates slower than non-diabetic ADSC (NGT). A, Growth curves for subcutaneous ADSC; B, growth curves for omental ADSC; C, number of subcutaneous ADSC present in G2/S phase of the cell cycle before (without FBS) and after (with FBS) stimulation by FBS for 24 h, D, number of omental ADSC present in G2/S phase before and after 24-hour stimulation by FBS. Shown are Means ± SEM, $n = 15$, Mann-Whitney U test. * - $p < 0.01$.

big lipid droplets (the data not shown). This trend was observed for both subcutaneous and omental adipocytes. Secondly, the ADSC adipogenic potential was measured quantitatively by the expression of adipogenic markers, *GLUT4*, *PPARgamma* and *FABP4*. The mRNA levels of these adipogenic markers were significantly 3–5-fold lower in both subcutaneous and omental adipocytes derived from diabetic ADSC than in non-

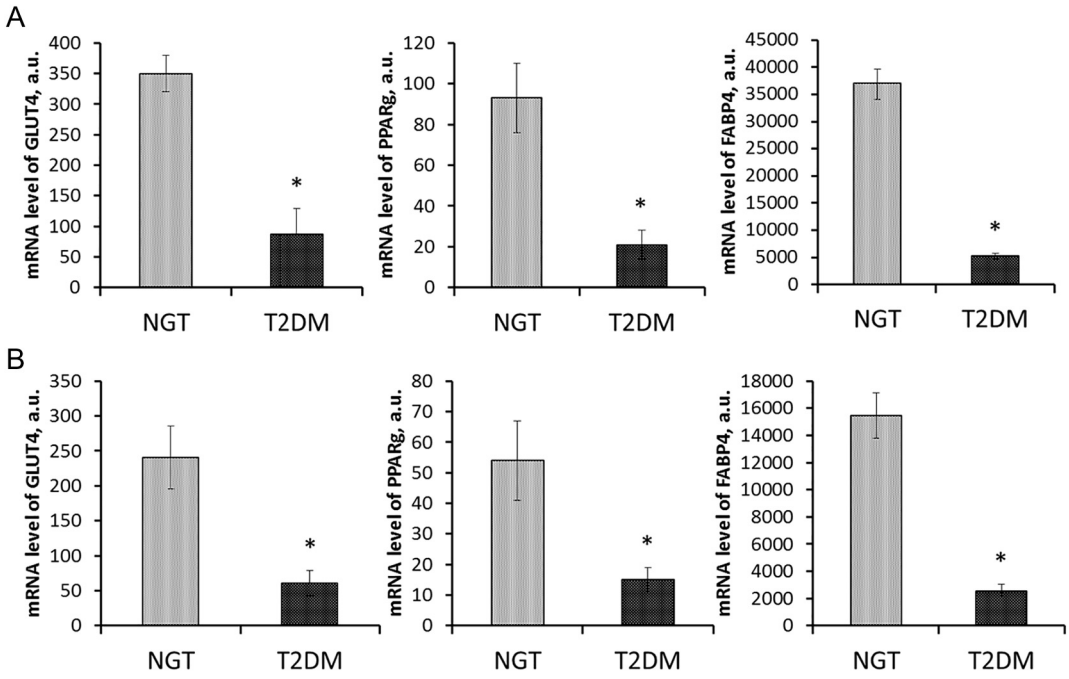

Fig. 3. Expression of adipogenic markers is lower in adipocytes derived from diabetic (T2DM) than non-diabetic (NGT) ADSC. A, relative expression of *GLUT4*, *PPARgamma* and *FABP4* in adipocytes derived from subcutaneous ADSC; B, relative expression of *GLUT4*, *PPARgamma* and *FABP4* in adipocytes derived from omental ADSC. The data are Mean ± SEM, $n = 15$, Mann-Whitney U test. * - $p < 0.01$.

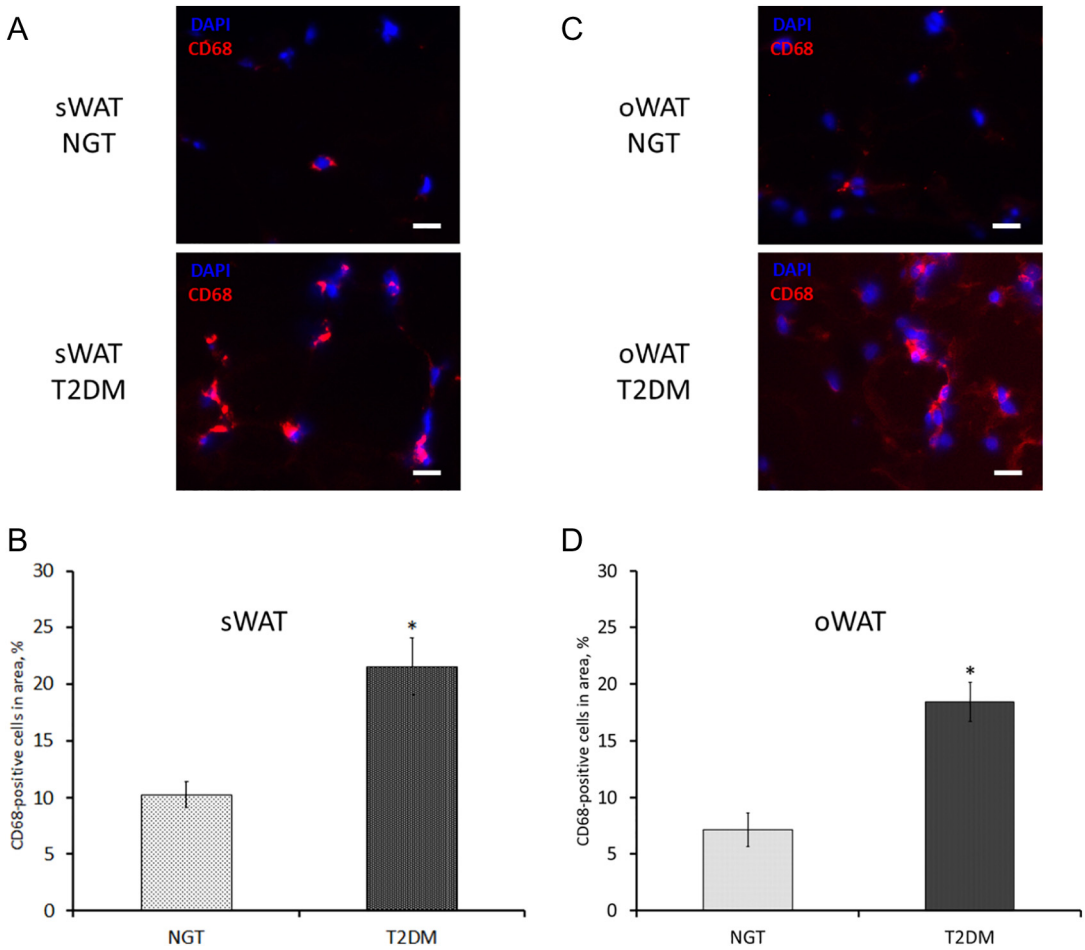

Fig. 4. Diabetic subcutaneous (sWAT, A and B) and omental (oWAT, C and D) fat is more infiltrated by CD68-positive macrophages than non-diabetic. The histological sections of diabetic (T2DM) and non-diabetic (NGT) white adipose biopsies were immunostained for CD68 and DAPI. A and C, representative images of sWAT and oWAT cryosections, respectively, B and D, corresponding statistical histograms of the number of CD68-positive cells; the data are Mean ± SEM, $n = 20$, Mann-Whitney U test. *$p < 0.01$, ** $0.01 < p < 0.05$. Scale bar = 40 μm.

diabetic ADSC (Fig. 3A,B). Thus, diabetic ADSC appear to have lower adipogenic activity as compared to healthy ADSC.

3.6. Diabetic fat is more infiltrated by CD68-positive macrophages

Adipocyte hypertrophy may be associated with increased inflammation. To test this possibility, we determined macrophage infiltration of subcutaneous and omental WAT biopsies of NGT and T2DM patients. Both T2DM tissues were found twice more infiltrated by CD68-positive cells as compared to non-diabetic NGT controls. The differences were about 2-fold for subcutaneous WAT (21.6% ± 2.5% vs. 10.3% ± 1.2% of $CD68^+$-positive cells, *$p < 0.01$, Mann-Whitney *U* test) (Fig. 4A,B), and 2.6-fold for omental WAT (18.4% ± 1.8% $CD68^+$-cells vs. 7.1% ± 1.5% $CD68^+$-cells, *$p < 0.01$, Mann-Whitney U test) (Fig. 4C,D). These results suggest that both diabetic fat tissues have increased inflammatory background.

3.7. Pro-inflammatory M1-like macrophages are similar in diabetic and non-diabetic fat

Because the in-tissue macrophages develop a spectrum of phenotypes ranging from the pro-inflammatory M1 type to the anti-inflammatory M2 type, we used common markers for M1-like and M2-like macrophages to assess their presence in diabetic and non-diabetic fat. Cryosections of subcutaneous and omental fat biopsies were immunostained for CCR7, which is one of the classic markers of pro-inflammatory M1-macrophages,[31,32] and CD68 to match the signal to macrophages. As shown in Fig. 5, the fraction of $CD68^+/CCR7^+$ M1-like macrophages was about 60% of all $CD68^+$-positive macrophages in both diabetic, and non-diabetic subcutaneous fat. In the omental fat, the M1-like macrophage content was about 80% and also did not differ between diabetic and non-diabetic biopsies. Thus, regardless of fat location infiltration by M1-like macrophages is similar in diseased and non-diabetic states.

3.8. Fraction of anti-inflammatory M2-like macrophages is less in diabetic than non-diabetic fat

To visualize M2-like macrophages in cryosections of fat biopsies we used CD206 marker, which is one of the classic markers of anti-inflammatory M2-macrophages.[31,32] Almost all CD68-positive macrophages were also positive for CD206 in both subcutaneous and omental non-diabetic fat of NGT patients indicating they have M2-like phenotype. The $CD68^+/CD206^+$ fraction of M2-like macrophages was less in diabetic biopsies, amounting for 85% in the subcutaneous and nearly 70% in the omental fat biopsies (Fig. 6). It should be noted that considering the increased total number of macrophages in diabetic fat (c.f. Fig. 4) the M2/M1 ratio is shifted towards inflammatory state (refer to Discussion for the details).

3.9. Increased activation of stress-activated kinases JNK1/2 in diabetic fat

Because activation of stress-activated MAP-kinases JNK1/2 reports inflammation and insulin resistance in obesity,[33] we measured phosphorylation of JNK1/2 on activatory sites in diabetic and non-diabetic adipocytes differentiated from both subcutaneous and omental ADSC.

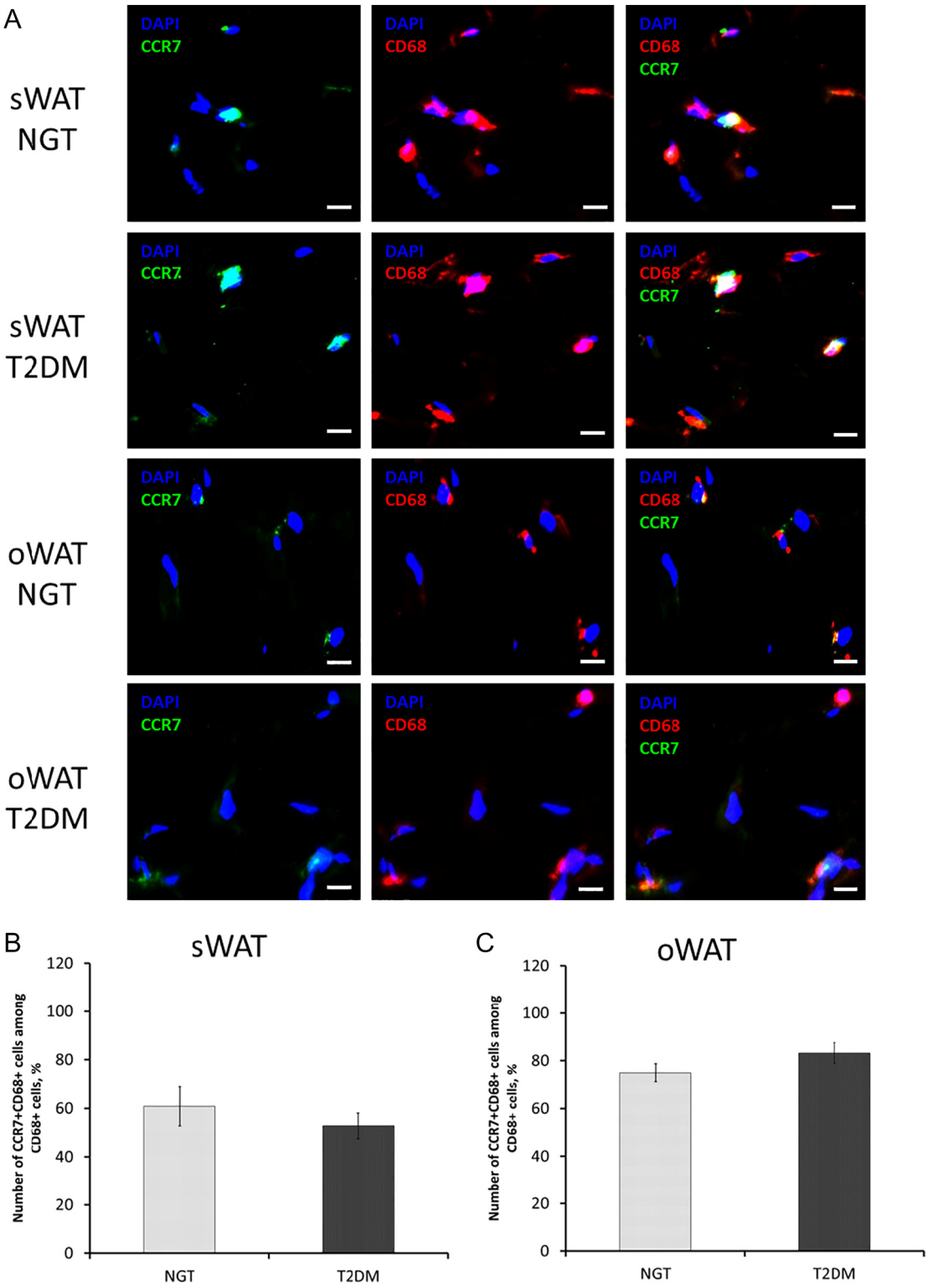

Fig. 5. Detection of M1-like macrophages in cryosections of subcutaneous (sWAT) and omental (oWAT) adipose biopsies. A, panel of images representing immunostaining of serial cryosections for CCR7 (green), CD68 (red), and nuclei (DAPI). B and C, statistical histograms of the fraction of $CCR7^{+}$ cells among all $CD68^{+}$-cells in the examined sWAT or oWAT images, respectively. The data in are Mean ± SEM, $n = 20$, Mann-Whitney U test. * - $p < 0.01$, ** - $0.01 < p < 0.05$. Scale bar = 20 μm.

The results of western blot are shown in Fig. 7. They demonstrate that activation JNK1/2 phosphorylation is significantly increased in both groups of diabetic adipocytes as compared to non-diabetic adipocytes. Thus, adipocytes grown from diabetic ADSC in culture seem to retain increased JNK1/2 phosphorylation, suggesting their upregulated stress/inflammatory state.

4. Discussion

The main question we asked in this study is what may drive IR development in people with long and morbid obesity, and why some of them do not develop T2DM while the others do. We compared biopsies from their subcutaneous and omental fat with regard to adipocyte

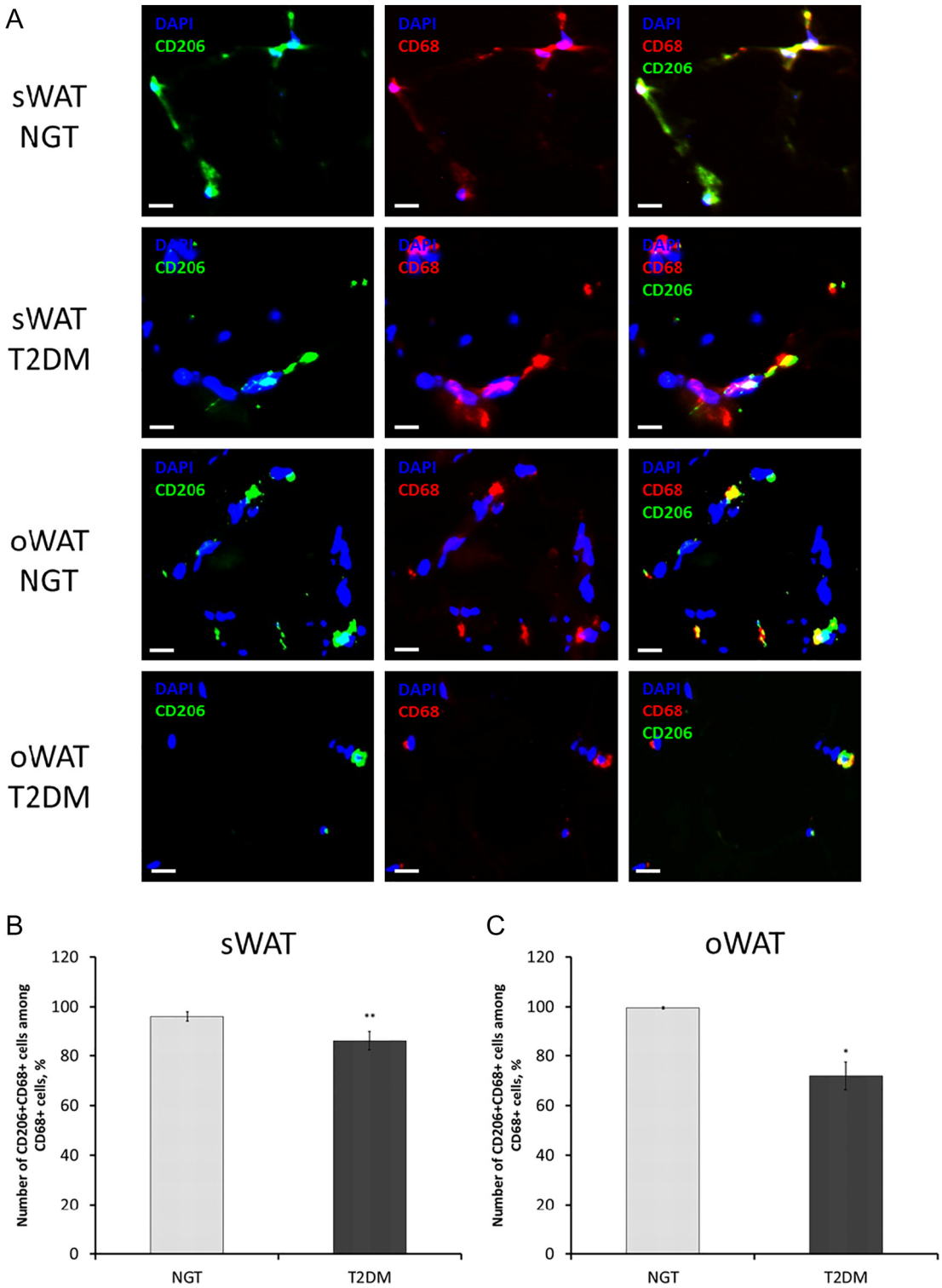

Fig. 6. Detection of M2-like macrophages in cryosections of subcutaneous (sWAT) and omental (oWAT) adipose biopsies. A, panel of images representing immunostaining of serial cryosections for CD206 (green), CD68 (red), and nuclei (DAPI). B and C, statistical histograms of the fraction of $CD206^{+}$-cells among all $CD68^{+}$-cells in the examined images of sWAT or oWAT, respectively. The data in are Mean ± SEM, $n = 20$, Mann-Whitney U test. * - $p < 0.01$, ** - $0.01 < p < 0.05$. Scale bar = 20 μm.

morphology, macrophage infiltration, inflammation state, and proliferation ability of the adipocyte precursor cells. We found that diabetic adipocytes are larger, their ADSC precursors proliferate slower and have decreased adipogenic potential, the diabetic fat is infiltrated by macrophages twice as much as non-diabetic along with increased M2/M1 macrophage ratio, and increased activity of the stress/inflammatory JNK1 pathway in diabetic vs. non-diabetic ADSC. We conclude that diabetic disease may be at least in part due to impaired renewal of healthy adipocytes, hypertrophy of the existing fat depots, increased macrophage infiltration and inflammation of the fat tissue, resulting in loss of insulin sensitivity and progression of T2DM, as summarized in Fig. 8.

We found that both subcutaneous and omental diabetic adipocytes are apparently hypertrophic because that display larger size than their

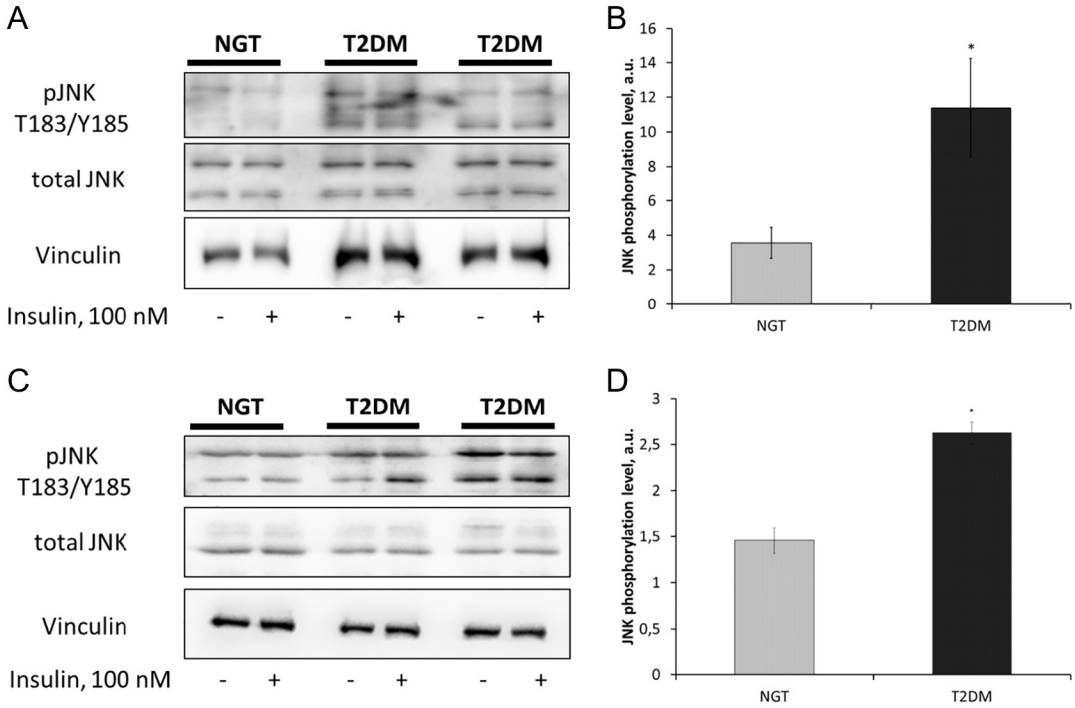

Fig. 7. Increased JNK1/2 phosphorylation in adult diabetic adipocytes. Both subcutaneous (A and B), and omental (C and D) adipocytes derived from the non-diabetic (NGT) and diabetic (T2DM) ADSC were assayed. Shown are the representative western membranes (A and C), and their quantified results (B and D). The data are Mean ± SEM, $n = 9$, Mann-Whitney U test. * - $p < 0.01$.

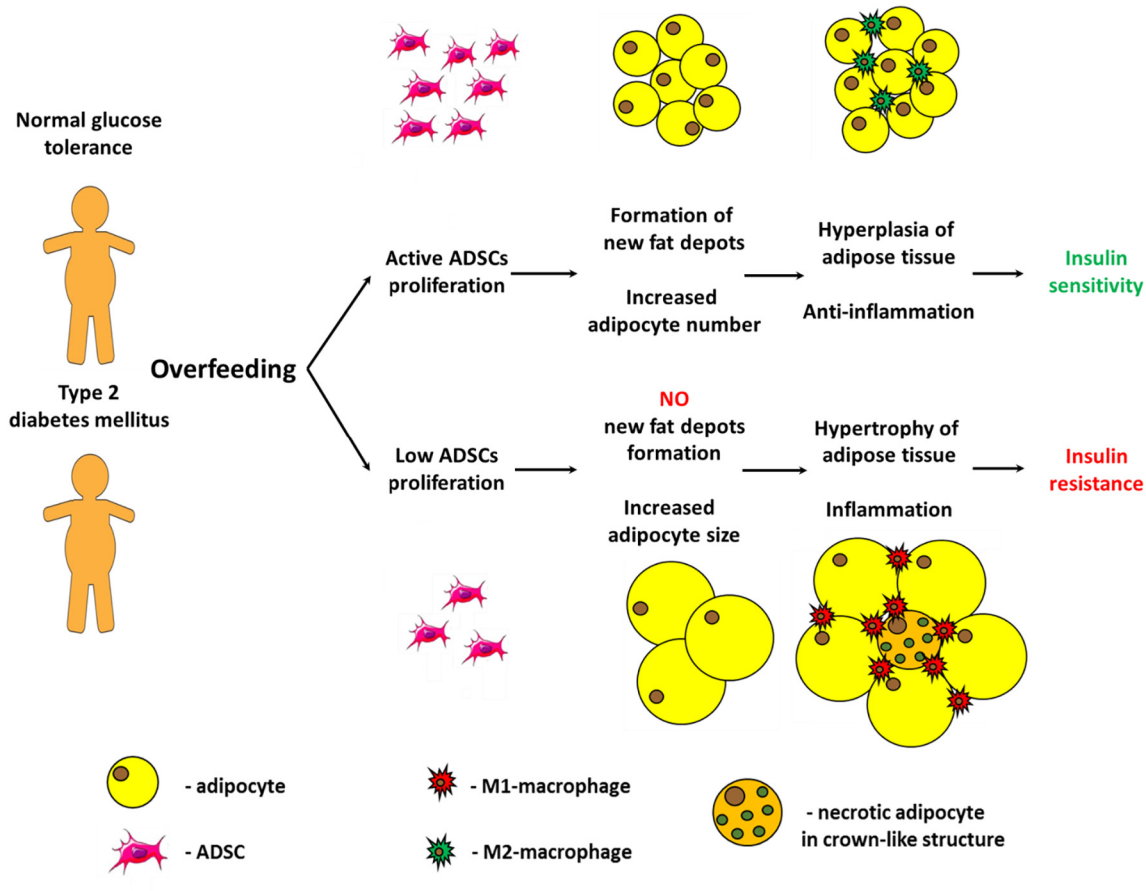

Fig. 8. Summary of the hypothesis and results obtained in this study. While overfeeding generally results in increased fat deposition in subcutaneous and visceral adipose tissues, the diabetic adipocytes are hypertrophied and proliferation of their precursor ADSC is compromised. This increases hypoxia and macrophage infiltration of diabetic fat, resulting in latent inflammation and insulin resistance, which is prerequisite for T2DM development.

non-diabetic counterparts (Fig. 1). The diabetic fat had less adipocytes in the same volume compared to metabolically healthy fat. It could have been because of a lower proliferative activity of adipogenic precursors in diseased fat. Therefore we tested this possibility and found that while serum stimulated proliferation of non-diabetic subcutaneous ADSC, it almost failed to increase proliferation of diabetic subcutaneous ADSC (Fig. 2A). Omental ADSC displayed similar trend, although the difference between diabetic and non-diabetic cells was delayed and less pronounced, reaching statistical significance after 72 h of stimulation. To justify these results, we analyzed cell distribution between phases of the cell cycle. After 24 h of stimulation, FBS significantly increased the number of healthy subcutaneous ADSC in the active G2/S state, whereas it had no effect on diabetic subcutaneous ADSC (Fig. 2C). This suggests that the differences seen in ADSC growth curves are due to reduced responsiveness of diseased cells to growth factors and cell cycle progression. Again, the increase in the omental cells being in G2/S phase was not significantly different between NGT and T2DM cells at 24 h of FBS stimulation (Fig. 2D), which is consistent with the delayed bifurcation of the cell growth curves (c.f. Fig. 2B).

The blunted proliferation of diabetic ADSC, lower adipogenic activity and expression of the key adipogenic markers (Fig. 3) are likely to result in a reduced capacity of new fat depot formation. It could be expected that under such circumstances the existing adipocytes become hypertrophied and resistant to insulin action. Whether intrinsic cellular mechanisms additional to those identified so far exist to govern the loss of insulin sensitivity due to exhaustion of lipid stores in hypertrophied adipocytes requires the future studies.

The adipocyte hypertrophy is a risk factor for hypoxia and latent inflammation in the fat tissue[9,10,34] via recruitment of macrophages and their differentiation into the pro-inflammatory phenotype.[6,35,36]. In turn, latent inflammation may also stimulate the adipocyte hypertrophy. Activation of inflammatory cascades during oxidative and endoplasmic reticulum stress in response to overnutrition may cause recruitment of M1-macrophages and other immune cells, which remodel extracellular matrix to create a niche for hypertrophied cell growth. Thus, the level of cathepsin K protease, which degrades fibronectin and collagens I and II, is found to be increased in obesity.[37] In addition, adipocyte hypertrophy is associated with altered levels of matrix metalloproteinase inhibitors.[38,39]

Macrophages are the most downstream immune cells which inflammatory profile reflects that of the upstream cells such as T-lymphocytes and innate lymphoid cells.[40–44] However, assessment of total macrophage infiltration gives only a rough estimate of fat inflammation because macrophages develop into either pro-, or anti-inflammatory phenotype.[45–48] Therefore we assessed whether the diabetic fat tissues contain more pro-inflammatory (M1-like) and/or less anti-inflammatory (M2-like) macrophages.

Using CCR7 as a marker of M1 macrophages we found that diabetic and non-diabetic adipose biopsies were not different in M1-like macrophage population, which was about 60% for subcutaneous and about 80% for the omental specimen. Almost all macrophages in non-diabetic fat biopsies displayed CD68 and CD206 markers of the M2 phenotype regardless of the fat origin, whereas only 85% and 70% of macrophages were M2-positive in diabetic subcutaneous and omental fat biopsies, respectively. However, taking into account that total number of macrophages is twice increased in diseased fat (Fig. 4), the fraction of pro-inflammatory M1-like macrophages is thus increased to 1.2 and 1.6 in diabetic subcutaneous and omental fat as compared to 0.6 and 0.8 in non-diabetic, respectively. Similarly, the fraction of anti-inflammatory M2-like macrophages is increased to 1.7 and 1.4 in diabetic subcutaneous and omental specimen, respectively, versus remaining 1 in the healthy fats. If to take the M1/M2 ratio as an estimate of the pro-inflammatory environment, it is 0.6/1 = 0.6 in non-diabetic subcutaneous fat versus 1.2/1.7 = 0,7 in diabetic subcutaneous fat. However, this difference is much bigger for the omental fat, where the M1/M2 ratio is 0.8/1 = 0.8 in non-diabetic vs. 1.6/1.4 = 1.14 in diabetic condition. Although rough, these estimates illustrate an increased pro-inflammatory background in diabetic patients, consistent with the well-established role of inflammation in IR development and T2DM progression.[49–53] In addition, these estimates are also consistent with the key pathogenic role of the omental fat, as it demonstrates much higher difference in the pro-inflammatory background (1.14/0.8 = 1.43) than subcutaneous fat (0.7/0.6 = 1.17). This is also consistent with clinical observations[54–57] and results of experimental studies.[58–60]

The inflammatory pathway mediated by stress-activated JNK1/2 MAP-kinases is upregulated in hypoxic environment and critically contributes to IR development in the fat tissue.[33,61–63] We assessed activation of JNK1/2 by phosphorylation level of its activatory T183/Y185 sites. It was significantly higher in both subcutaneous and omental adipocytes differentiated from ADSC of diabetic patients as compared to non-diabetic adipocytes (Fig. 7). This is consistent with the increased pro-inflammatory background in diabetic fat and higher IR as determined by the hyperinsulinemic-euglycemic clamp test in diabetic patients.

5. Conclusions

We report here that diabetic ADSC have impaired proliferation associated with the in situ hypertrophy of adult adipocytes and increased inflammatory background in subcutaneous and omental fat. In the context of T2DM pathogenesis, these conditions not only favor increased IR, which was confirmed by hyperinsulinemic-euglycemic clamp test in diabetic patients, but also likely prevent formation of new fat depots from ADSC, which could be capable of counteracting IR (Fig. 8). This is consistent with altered expression of adipogenic genes and adipogenesis associated with pathogenesis of T2DM,[64–67] which may provide still a missing link between the ADSC dysfunction observed in this study, and T2DM progression in obese individuals.

Conflict of interest

The authors declare no conflict of interest.

Acknowledgments

Authors are grateful to colleagues from the M.V. Lomonosov Moscow State University, Department of Biochemistry and Molecular Medicine (Dr. K.Kulebyakin, Dr. P.Tyurin-Kuzmin and Mrs. A.Stepanova) for the fruitful discussion of the working hypothesis that was conceived independently by the both groups.

Funding

This study was supported by Russian Science Foundation (RSF grant no. 17-15-01435).

References

1. Eckel RH, Kahn SE, Ferrannini E, Goldfine AB, Nathan DM, Schwartz MW, et al. Obesity and type 2 diabetes: what can be unified and what needs to be individualized. J Clin Endocrinol Metab 2011;34:1424-30, https://doi.org/10.1210/jc.2011-0585.
2. Shoelson SE, Lee J, Goldfine AB. Inflammation and insulin resistance. J Clin Invest 2006;116:1793-801, https://doi.org/10.1172/JCI29069.
3. Sears B, Perry M. The role of fatty acids in insulin resistance. Lipids Health Dis 2015;14, 121, https://doi.org/10.1186/s12944-015-0123-1.
4. Henriksen EJ, Diamond-Stanic MK, Marchionne EM. Oxidative stress and the etiology of insulin resistance and type 2 diabetes. Free Radic Biol Med 2011;51:993-9, https://doi.org/10.1016/j.freeradbiomed.2010.12.005.
5. Scheuner D, Kaufmann RJ. The unfolded protein response: a pathway that links insulin demand with β-cell failure and diabetes. Endocr Rev 2008;29:317-33, https://doi.org/10.1210/er.2007-0039.
6. Stafeev IS, Vorotnikov AV, Ratner EI, Menshikov MY, Parfyonova YV. Latent inflammation and insulin resistance in adipose tissue. Int J Endocrinol 2017;2017:1-12, https://doi.org/10.1155/2017/5076732.

7. Ozcan U, Cao Q, Yilmaz E, Lee AH, Iwakoshi NN, Ozdelen E, et al. Endoplasmic reticulum stress links obesity, insulin action, and type 2 diabetes. Science 2004;306:457-61, https://doi.org/10.1126/science.1103160.
8. Houstis N, Rosen ED, Lander ES. Reactive oxygen species have a causal role in multiple forms of insulin resistance. Nature 2006;440:944-8, https://doi.org/10.1038/nature04634.
9. Trayhurn P. Hypoxia and adipose tissue function and dysfunction in obesity. Physiol Rev 2013;93:1-21, https://doi.org/10.1152/physrev.00017.2012.
10. Yang J, Eliasson B, Smith U, Cushman SW, Sherman AS. The size of large adipose cells is a predictor of insulin resistance in first-degree relatives of type 2 diabetic patients. Obesity (Silver Spring) 2012;20:932-8, https://doi.org/10.1038/oby.2011.371.
11. Kern PA, Ranganathan S, Li C, Wood S, Ranganathan G. Adipose tissue tumor necrosis factor and interleukin-6 expression in human obesity and insulin resistance. Am J Physiol Endocrinol Metab 2001;280:E745-51, https://doi.org/10.1152/ajpendo.2001.280.5.E745.
12. Spranger J, Kroke A, Möhlig M, Hoffmann K, Bergmann MM, Ristow M, et al. Inflammatory cytokines and the risk to develop type 2 diabetes: results of the prospective population-based European Prospective Investigation into Cancer and Nutrition (EPIC)-Potsdam Study. Diabetes 2003;52:812-7, https://doi.org/10.2337/diabetes.52.3.812.
13. Salmenniemi U, Ruotsalainen E, Pihlajamäki J, Vauhkonen I, Kainulainen S, Punnonen K, et al. Multiple abnormalities in glucose and energy metabolism and coordinated changes in levels of adiponectin, cytokines and adhesion molecules in subjects with metabolic syndrome. Circulation 2004;110:3842-8, https://doi.org/10.1161/01.CIR.0000150391.38660.9B.
14. Le K-A, Mahurkar S, Alderete TL, Hasson RE, Adam TA, Kim JS, et al. Subcutaneous adipose tissue macrophage infiltration is associated with hepatic and visceral fat deposition, hyperinsulinemia, and stimulation of NF-kB stress pathway. Diabetes 2011;60:2802-9, https://doi.org/10.2337/db10-1263.
15. McLaughlin T, Liu L-F, Lamendola C, Shen L, Morton J, Rivas H, et al. T-cell profile in adipose tissue is associated with insulin resistance and systemic inflammation in humans. Arterioscler Thromb Vasc Biol 2015;34:2637-43, https://doi.org/10.1161/ATVBAHA.114.30463.
16. Bertola A, Ciucci T, Rousseau D, Bourlier V, Duffaut C, Bonnafous S, et al. Identification of adipose tissue dendritic cells correlated with obesity-associated insulin-resistance and inducing Th17 responses in mice and patients. Diabetes 2012;61:2238-47, https://doi.org/10.2337/db11-1274.
17. Adabimohazab R, Garfinkel A, Milam EC, Frosch O, Mangone A, Convit A. Does inflammation mediate the association between obesity and insulin resistance? Inflammation 2016;39:994-1003, https://doi.org/10.1007/s10753-016-0329-z.
18. McIntosh K, Zvonic S, Garrett S, Mitchell JB, Floyd ZE, Hammill L, et al. The immunogenicity of human adipose-derived stem cells: temporal changes in vitro. Stem Cells 2006;24:1246-53, https://doi.org/10.1634/stemcells.2005-0235.
19. Melief SM, Zwaginga JJ, Fibbe WE, Roelofs H. Adipose tissue-derived multipotent stromal cells have a higher immunomodulatory capacity than their bone marrow-derived counterparts. Stem Cells Transl Med 2013;2:455-63, https://doi.org/10.5966/sctm.2012-0184.
20. Russo V, Yu C, Belliveau P, Hamilton A, Flynn LA. Comparison of human adipose-derived stem cells isolated from subcutaneous, omental and intrathoracic adipose tissue depots for regenerative applications. Stem Cells Transl Med 2014;3:206-17, https://doi.org/10.5966/sctm.2013-0125.
21. Shang Q, Bai Y, Wang G, Song Q, Guo C, Zhang L, et al. Delivery of adipose-derived stem cells attenuates adipose tissue inflammation and insulin resistance in obese mice through remodeling macrophage phenotypes. Stem Cells Dev 2015;24:2052-64, https://doi.org/10.1089/scd.2014.0557.
22. Cao M, Pan Q, Dong H, Yuan X, Li Y, Sun Z, et al. Adipose-derived mesenchymal stem cells improve glucose homeostasis in high-fat diet-induced obese mice. Stem Cells Res Ther 2015;6, 208, https://doi.org/10.1186/s13287-015-0201-3.
23. Liao N, Zheng Y, Xie H, Zhao B, Zeng Y, Liu X, et al. Adipose tissue-derived stem cells ameliorate hyperglycemia, insulin resistance and liver fibrosis in the type 2 diabetic rats. Stem Cells Res Ther 2017;8, 286, https://doi.org/10.1186/s13287-017-0743-7.
24. Zhao H, Shang Q, Pan Z, Bai Y, Li Z, Zhang H, et al. Exosomes from adipose-derived stem cells attenuate adipose inflammation and obesity through polarizing M2 macrophages and beiging in white adipose tissue. Diabetes 2018;67:235-47, https://doi.org/10.2337/db17-0356.
25. Conleya SM, Zhua XY, Eirina A, Tanga H, Lermanb A, van Wijnenc AJ, et al. Metabolic syndrome alters expression of insulin signaling-related genes in swine mesenchymal stem cells. Gene 2018;644:101-6, https://doi.org/10.1016/j.gene.2017.10.086.
26. Pincu Y, Huntsman HD, Zou K, De Lisio M, Mahmassani ZS, Munroe MR, et al. Diet-induced obesity regulates adipose-resident stromal cell quantity and extracellular matrix gene expression. Stem Cell Res 2016;17:181-90, https://doi.org/10.1016/j.scr.2016.07.002.
27. Eljaafari A, Robert M, Chehimi M, Chanon S, Durand C, Vial G, et al. Adipose tissue–derived stem cells from obese subjects contribute to inflammation and reduced insulin response in adipocytes through differential regulation of the Th1/Th17 balance and monocyte activation. Diabetes 2015;64:2477-88, https://doi.org/10.2337/db15-0162.
28. Zebisch K, Voight V, Wabitsch M, Brandsch M. Protocol for effective differentiation of 3T3L1 cells to adipocytes. Anal Biochem 2012;425:88-90, https://doi.org/10.1016/j.ab.2012.03.005.
29. Laemmli UK. Cleavage of structural proteins during the assembly of the head of bacteriophage T4. Nature 1970;15:680-5.
30. De Fronzo RA, Tobin JD, Andres R. Glucose clamp technique: a method for quantifying insulin secretion and resistance. Am J Physiol 1979;237:E214-23, https://doi.org/10.1152/ajpendo.1979.237.3.E214.
31. Martinez FO, Gordon S, Locati M, Mantovani A. Transcriptional profiling of the human monocyte-to-macrophage differentiation and polarization: new molecules and patterns of gene expression. J Immunol 2006;177:7303-11, https://doi.org/10.4049/jimmunol.177.10.7303.
32. Xuan W, Qu Q, Zheng B, Xiong S, Fan GH. The chemotaxis of M1 and M2 macrophages is regulated by different chemokines. J Leukoc Biol 2015;97:61-9, https://doi.org/10.1189/jlb.1A0314-170R.
33. Hirosumi J, Tunchman G, Chang L, Gorgun CZ, Uysal KT, Maeda K, et al. A central role for JNK in obesity and insulin resistance. Nature 2002;420:333-6, https://doi.org/10.1038/nature01137.
34. Stafeev IS, Menshikov MY, Tsokolaeva ZI, Shestakova MV, Parfyonova YV. Molecular mechanisms of latent inflammation in metabolic syndrome. Possible role of sirtuins and peroxisome proliferator-activated receptor type gamma. Biochemistry (Mosc) 2015;80:1217-26, https://doi.org/10.1134/S0006297915100028.
35. Boutens L, Stienstra R. Adipose tissue macrophages: going off track during obesity. Diabetologia 2016;59:879-94, https://doi.org/10.1007/s00125-016-3904-9.
36. Vieira-Potter V. Inflammation and macrophage modulation in adipose tissues. Cell Microbiol 2014;16:1484-92, https://doi.org/10.1111/cmi.12336.
37. Taleb S, Cancello R, Clement K, Lacasa D. Cathepsins promotes human preadipocyte differentiation: possible involvement of fibronectin degradation. Endocrinology 2006;147:4950-9, https://doi.org/10.1210/en.2006-0386.
38. Chun TH. Peri-adipocyte ECM remodeling in obesity and adipose tissue fibrosis. Adipocyte 2012;1:89-95, https://doi.org/10.4161/adip.19752.
39. Lin D, Chun TH, Kang L. Adipose extracellular matrix remodeling in obesity and insulin resistance. Biochem Pharmacol 2016;119:8-16, https://doi.org/10.1016/j.bcp.2016.05.005.
40. Saetang J, Sangkhathat S. Role of innate lymphoid cells in obesity and metabolic diseases. Mol Med Rep 2018;17:1403-12, https://doi.org/10.3892/mmr.2017.8038.
41. Boulenovar S, Michelet X, Duquette D, Alvarez D, Hogan AE, Dold C, et al. Adipose type one innate lymphoid cells regulate macrophage homeostasis through targeted cytotoxicity. Immunity 2017;46:273-86, https://doi.org/10.1016/j.immuni.2017.01.008.
42. O'Sullivan TE, Rapp M, Fan X, Weizmann O-E, Bhardwaj P, Adams NM, et al. Adipose-resident group 1 innate lymphoid cells promote obesity-associated insulin resistance. Immunity 2017;45:428-41, https://doi.org/10.1016/j.immuni.2016.06.016.
43. Molofsky AB, Nussbaum JC, Liang H-E, Van Dyken SJ, Cheng LE, Mohapatra A, et al. Innate lymphoid type 2 cells sustain visceral adipose tissue eosinophils and alternatively activated macrophages. J Exp Med 2013;210:535-49, https://doi.org/10.1084/jem.20121964.
44. Cautivo KM, Molofsky AB. Regulation of metabolic health and adipose tissue function by group 2 innate lymphoid cells. Eur J Immunol 2016;46:1315-25, https://doi.org/10.1002/eji.201545562.
45. Catrysse L, Van Loo G. Adipose tissue macrophages and their polarization in health and obesity. Cell Immunol 2018;330:114-9, https://doi.org/10.1016/j.cellimm.2018.03.001.
46. Fujisaka S, Usui I, Bukhari A, Ikutani M, Oya T, Kanatani Y, et al. Regulatory mechanisms for adipose tissue M1 and M2 macrophages in diet-induced obese mice. Diabetes 2009;58:2574-82, https://doi.org/10.2337/db08-1475.
47. Morris DL, Singer K, Lumeng CN. Adipose tissue macrophages: phenotypic plasticity and diversity in lean and obese states. Curr Opin Clin Nutr Metab Care 2011;14:341-6, https://doi.org/10.1097/MCO.0b013e328347970b.
48. Hill AA, Reid Bolus W, Hasty AH. A decade of progress in adipose tissue macrophage biology. Immunol Rev 2014;262:134-52, https://doi.org/10.1111/imr.12216.
49. Wellen KE, Hotamisligil GS. Obesity-induced inflammatory changes in adipose tissue. J Clin Invest 2003;112:1785-7, https://doi.org/10.1172/JCI20514.
50. Wellen KE, Hotamisligil GS. Inflammation, stress and diabetes. J Clin Invest 2005;115:1111-9, https://doi.org/10.1172/JCI25102.
51. Hotamisligil GS. Inflammation and metabolic disorders. Nature 2006;444:860-7, https://doi.org/10.1038/nature05485.
52. Kohlgruber A, Lynch L. Adipose tissue inflammation in the pathogenesis of type 2 diabetes. Curr Diab Rep 2015;15, 92, https://doi.org/10.1007/s11892-015-0670-x.
53. Richardson VR, Smith KA, Carter AM. Adipose tissue inflammation: feeding the development of type 2 diabetes mellitus. Immunobiology 2013;218:1497-504, https://doi.org/10.1016/j.imbio.2013.05.002.
54. Corominola H, Conner LJ, Beavers LS, Gadski RA, Johnson D, Caro JF, et al. Identification of novel genes differentially expressed in omental fat of obese subjects and obese type 2 diabetic patients. Diabetes 2001;50:2822-30, https://doi.org/10.2337/diabetes.50.12.2822.
55. Ghansah T, Murr M, Watson JE, Yoder S, Fleming D, Nelson N, et al. Mesenteric and omental depot differences in fat tissue inflammatory markers and signaling from type 2 diabetic (T2D) and normal obese humans. FASEB J 2011;25.
56. Tordjman J, Poitou C, Hugol D, Bouillot JL, Basdevant A, Bedossa P, et al. Association between omental adipose tissue macrophages and liver histopathology in morbid obesity: influence of glycemic status. J Hepatol 2009;51:354-62, https://doi.org/10.1016/j.jhep.2009.02.031.
57. Poulain-Godefroy O, Lecoeur C, Pattou F, Fruhbeck G, Froguel P. Inflammation is associated with a decrease of lipogenic factors in omental fat in women. Am J Physiol Regul Integr Comp Physiol 2008;295:R1-7, https://doi.org/10.1152/ajpregu.00926.2007.
58. Garcia-Ruiz I, Solis-Munoz P, Fernandez-Moreira D, Grau M, Munoz-Yague MT, Solis-Herruzo JA. Omentectomy prevents metabolic syndrome by reducing appetite and body weight in a diet induced obesity rat model. Sci Rep 2018;8, 1540, https://doi.org/10.1038/s41598-018-19973-z.
59. Macdougall CE, Wood EG, Loschko J, Scagliotti V, Cassidy FC, Robinson ME, et al. Visceral adipose tissue immune homeostasis is regulated by the crosstalk between adipocytes and dendritic cell subsets. Cell Metab 2018;27:588-601, https://doi.org/10.1016/j.cmet.2018.02.007.
60. Coats BR, Schoenfelt KQ, Barbosa-Lorenzi VC, Peris E, Cui C, Hoffman A, et al. Metabolically activated adipose tissue macrophages perform detrimental and beneficial

functions during diet-induced obesity. Cell Rep 2017;20:3149-61, https://doi.org/10.1016/j.celrep.2017.08.096.
61. Aguirre V, Uchida T, Yenush L, Davis R, White MF. The c-Jun NH2-terminal kinase promotes insulin resistance during association with insulin receptor substrate 1 and phosphorylation of Ser(307). J Biol Chem 2000;275:9047-54, https://doi.org/10.1074/jbc.275.12.9047.
62. Solinas G, Karin M. JNK1 and IKKbeta: molecular links between obesity and metabolic dysfunction. FASEB J 2010;24:2596-611, https://doi.org/10.1096/fj.09-151340.
63. Solinas G, Becattini B. JNK at the crossroad of obesity, insulin resistance and cell stress response. Mol Metab 2017;6:174-84, https://doi.org/10.1016/j.molmet.2016.12.001.
64. Dubois SG, Heilbronn LK, Smith SR, Albu JB, Kelley DE, Ravussin E. Decreased expression of adipogenic genes in obese subjects with type 2 diabetes. Obesity (Silver Spring) 2006;14:1543-52, https://doi.org/10.1038/oby.2006.178.
65. Gustafson B, Hedjazifar S, Gogg S, Hammarstedt A, Smith U. Insulin resistance and impaired adipogenesis. Trends Endocrinol 2015;26:193-200, https://doi.org/10.1016/j.tem.2015.01.006.
66. Isakson P, Hammarstedt A, Gustafson B, Smith U. Impaired preadipocyte differentiation in human abdominal obesity: role of Wnt, tumor necrosis factor alpha and inflammation. Diabetes 2009;58:1550-7, https://doi.org/10.2337/db08-1770.
67. Arner P, Arner E, Hammarstedt A, Smith U. Genetic predisposition for type 2 diabetes, but not for overweight/obesity, is associated with a restricted adipogenesis. PLoS One 2011;12, e18284, https://doi.org/10.1371/journal.pone.0018284.